

Monolithic column plastic microfluidic device for peptide analysis using electrospray from a channel opening on the edge of the device

Jian Liu, Kyung-Won Ro, Ranu Nayak, Daniel R. Knapp*

*Department of Cell and Molecular Pharmacology and Experimental Therapeutics, Medical University of South Carolina,
173 Ashley Avenue, Charleston, SC 29425, United States*

Received 20 June 2006; received in revised form 21 August 2006; accepted 28 August 2006
Available online 25 September 2006

Abstract

Electrospray from a channel exit at the edge of a fluorocarbon coated cycloolefin copolymer microfluidic device has been investigated. The fluorocarbon coating facilitated generation of a stable electrospray, thereby enhancing the detectability of electrospray ionization (ESI) mass spectrometry (MS). A microfluidic device of integrated ESI emitters and monolithic liquid chromatography columns has been fabricated on a cycloolefin copolymer chip. The monolithic columns were polymerized in situ using UV irradiation with a photomask to confine the porous polymer monolith to the desired regions of the channels. The monolithic stationary phase was homogenous and well bonded to the channel surfaces, which had been functionalized by graft polymerization. The ESI potential was applied within the channel via a carbon ink line. The performance of this microfluidic device was demonstrated by analysis of a tryptic digest of bovine serum albumin on an ion trap MS instrument.
© 2006 Elsevier B.V. All rights reserved.

Keywords: Electrospray ionization; Mass spectrometry; Monolithic column; Plastic microfluidic device

1. Introduction

Improving the efficiency of various sampling techniques for peptide and protein analysis by mass spectrometry and tandem mass spectrometry has had a vital role in the expansion of the field of proteomics. A primary problem in proteomics is the detection of low abundance proteins in a complex matrix. Interfacing high-resolution separation and ion introduction techniques to mass spectrometry is key to meeting this requirement. Electrospray ionization is one of the major methods for generating charged ions of proteins and peptides for mass spectrometric analysis. Robust, low flow rate, and highly efficient ESI emitters have shown advantages in performing proteomic studies using mass spectrometry for detecting low absolute amounts of analytes in biological samples [1–3].

Sheathless ESI is easily interfaced to low flow rate infusion or low flow rate separation techniques such as capillary electrophoresis, capillary electrochromatography, and nanoliquid chromatography [4]. For this kind of ESI emitter, two important

properties are a low liquid flow rate and the sharpness of the emitter. A low flow rate results in an high ionization efficiency and a sharp emitter leads to high electric field strength, which in turn means that lower voltages can be used at equal ionization efficiencies [5]. These characteristics of ESI have led to increasing interest in the manufacture of microfluidic devices with ESI emitters [6].

Inserting a capillary emitter into a chip channel is a commonly used method to fabricate a chip-based ESI emitter. However, it involves manual work and is therefore not convenient for batch production [7]. Many novel microfabrication techniques have been applied to develop state-of-the-art electrospray and nanospray emitters. Xie et al. [8,9] integrated a Parylene free-standing sharp ESI nozzle to an on-chip dispensing system by a sophisticated multi-layer deposition, releasing, and etching procedure. The performance characteristics of the needle-like polymer structures are very similar to conventional pulled fused silica or glass capillaries. Stable ion emission can be achieved at low nanoliters per minute flow rates, with applied potentials between 1 and 2 kV, over a period of a few hours [10]. An on-chip micro-nib device has also been developed as a nanospray emitter. With minimized slot width of the nib, the high voltage needed for generating a stable ESI was significantly reduced.

* Corresponding author. Tel.: +1 843 792 5830; fax: +1 843 792 2475.
E-mail address: knappdr@musc.edu (D.R. Knapp).

The reliability and the robustness are comparable to the standard needle sources [11,12]. Yang et al. sandwiched parylene electro-spray tips between the cycloolefin polymer plates of microfluidic channels with a gold electrode. The triangle-shaped hydrophilic parylene electro-spray tips were fabricated by photolithography and reactive ion etching methods. This microfabricated system showed a stable electro-spray performance [13,14].

Electrospray has also been demonstrated from the end of open channels in a PMMA wafer that exit at points on the periphery of the wafer [15]. Electrospray from channel exits with different point angles (30° , 60° , 90° , 120°) showed no significant difference in the ion signal stability or the onset voltage of the electro-spray. It appeared that the width of the channel exit determined the size of the Taylor cone, and that the sharpness of the tip had no significant influence on the electro-spray. This report would suggest that emitters that generate electro-spray from the exit of a channel on a flat edge could give good performance comparable to traditional pointed ESI emitters. Rohner et al. [16] developed a microspray emitter consisting of a channel opening on the edge of the device fabricated by photoablation of hydrophobic PET substrates. This emitter provided a highly stable and durable spray ionization. However, wetting of the edge led to an expanded Taylor cone. As a result, a wide-based Taylor cone formed on the unmodified flat edge away from the channel exit, which required a high voltage of 7–8 kV to obtain the best stability and the highest intensity of the base peak. Lozano et al. [17] demonstrated that ESI can be generated from flat edge. They showed that if the emitter material has low dielectric constant then the local electric field near the emission site is enhanced in a very similar way as with sharp metallic needles. Combining the nonwetting property of the material and the sharp corner formed in the hole–surface interface effectively anchors the Taylor cone to the edge of the hole, thus simplifying the process of emitter manufacturing.

Porous polymer monolith (PPM) assisted electro-spray ionization has been interfaced to mass spectrometry [18]. In this configuration, a PPM is formed at the flat end of a capillary to perform electro-spray ionization mass spectrometry presumably from multiple channel openings in the monolith. Stable electro-sprays are obtained at a variety of flow rates ranging from a few nanoliters to $1 \mu\text{L}/\text{min}$ for protein solutions at low concentrations. Mass spectra were obtained from as little a few femtomoles of material with good signal-to-noise ratio. An additional advantage of the PPM-filled capillary is that it is very robust and shows little loss in performance with use over extended periods of time.

Coating the edge surface of the microchip with a hydrophobic reagent helps reduce wetting of the chip edge to generate a stable electro-spray and reduces potential cross contamination among the channels [19]. Applying fluorocarbon material to the surface around emitter exit is a well-accepted strategy to enhance the hydrophobicity and reduce the electro-spray degradation by solvent wetting effect. Wang et al. [20] confined electro-spray from the flat edges of planar microfluidic chips by bonding hydrophobic PTFE membranes to the exit surfaces. The PTFE membrane consistently achieved well-defined and stable Taylor cone with no lateral spreading on PC substrates. Tang et al. [21] treated the surface of the microchip with a CF_4 RF plasma after the

spray emitter array was fabricated. The increased hydrophobicity of the treated polycarbonate surface prevented the sample solution from spreading over the edge of the emitter well and afforded stable electro-sprays from each emitter. Schilling et al. [22] fabricated a polymer nozzle for ESI-MS using a CNC jig-milling machine on a PMMA chip. The nozzle was modified by painting a solution of amorphous fluorine polymer to form a more hydrophobic surface. A well-formed Taylor cone on a fluoropolymer treated nozzle was obtained. However, instability and the degradation of the fluoropolymer coating was observed resulting in deterioration of the electro-spray efficiency and the lifetime of emitters. More recently, Jeyaprakash et al. [23] reported a novel surface modification method by covalently anchoring fluorinated polymer nanofilms onto micronozzle surfaces through a simple photochemical process. The modified surface eliminates fluctuations in the dispensed volume and allows delivery of nanoliters droplets, even of low surface tension liquids, in a highly reproducible manner. In summary, several reports indicate that treating the surface around the open-exit on a flat edge to make it hydrophobic improves electro-spray performances and preserves the efficiency of separation by reducing the wetting of the chip edge. However, there remains the potential for stability of the coating being affected by electrical discharge [6].

Applying the high electro-spray voltage through a conductor near the emitter nozzle requires careful consideration of electrochemical properties, conductivities, and durability of the conductor material. Comparing different conductive materials, chronoamperometric results indicated that the graphite coated nanospray emitter showed better electrochemical stabilities than the corresponding noble metal coated emitters [24]. The graphite coated emitter tip designed by Dahlin et al. [25] showed excellent electrochemical stability and durability allowing electro-spray for more than 180 h. This suggests that carbon-based electrodes are optimal for connecting the ESI potential.

Since the first report by Yates' group of multidimensional protein identification technology for shotgun proteomics [26,27], multiple separation techniques have been combined and interfaced to mass spectrometry to achieve high resolution and detectability. To reduce interface dead volume, Yang et al. [28] sealed two commercial uncoated New Objective electro-spray tips into the microchannels to integrate with an in situ polymerized monolithic bed and coupled to an ion trap mass spectrometer. Le Gac et al. [29] integrated a planar nib-like emitter with a monolithic column to perform separation and electro-spray ionization. A compact and versatile modular nanoLC–chip system has been reported by Yin et al. [30] and is now available as a commercial product (Agilent HPLC–chip-MS). A polyimide film is laser-ablated to form microfluidic channels, ports, chambers, and columns. A gold layer is electrodeposited near the electro-spray tip for contacts to the fluid flow channel prior to lamination of a cover layer to form closed channels. The integration of the precolumn, analytical column, and nanoelectrospray emitter in a compact format minimizes transfer lines and connections and reduces postcolumn peak broadening and dead volumes. This system provided good reproducibility of retention time and peak intensity. The modular concept of the microfluidic systems

also facilitated the integration of two-dimensional chromatography (strong cation exchange/C₁₈) thereby increasing the sample loading and selectivity of the nanoLC–chip-MS system.

With increasing interest in plastic microfluidic devices for proteomic analysis, there is need for methods of low cost micro-fabrication of disposable plastic microfluidic analytical devices to integrate ESI emitters and chromatographic columns. Here we report the fabrication of an ESI emitter for spraying from a channel opening on the edge of the device and the integration of this microfluidic emitter with a monolithic column on a chip for achieving high sensitivity MS detection while maintaining the resolution of liquid chromatography.

2. Experimental

2.1. Materials and chemicals

The cycloolefin copolymer (COC), Zeonor[®] 1020R (Zoen Chemicals L.P., Louisville, KY), was used as chip substrate material. Epoxy-based conductive carbon ink (C-100, Conductive Compounds, Inc., Londonderry, NH) was purchased from manufacturer. Glassy carbon spherical powder (type 2, 0.4–12 μm, Alfa Aesar, MA) was used to prepare in-house made conductive carbon ink. Fused-silica capillary (50 μm i.d., 150 μm o.d.) with polyimide coating was from Polymicro-Technologies (Phoenix, AZ). Perfluoroalkyl ether (Krytox 1625) was from Dupont (Wilmington, DE). Pico Tip[®] nanospray emitters (FS360-50-8-CE; 8 μm orifice) were purchased from New Objective (Woburn, MA).

Dithiothreitol, trypsin (proteomics grade), and bovine serum albumin (BSA) were purchased from Sigma (St. Louis, MO, USA). Trimethylolpropane triacrylate (TMPTA), ethylene diacrylate (EDA), benzophenone, ethylhexyl methacrylate (EHMA), ethylene glycol dimethacrylate (EDMA), 1-decanol, 2,2-dimethoxy-2-phenylacetophenone (DPA), dithiothreitol (DTT), iodoacetamide, and methylcyclohexane were purchased from Aldrich (Milwaukee, WI). Double distilled water was used. Trifluoroacetic acid (TFA), trichloroacetic acid (TCA), acetonitrile, acetone, methanol, ammonium bicarbonate and basic alumina were obtained from Fisher Scientific (Pittsburgh, PA). EHMA and EDMA were prepared by passing through basic alumina to remove the inhibitors. The other materials were used without further purification. The in house constructed UV irradiation chamber used in this work consisted of an array of five 8-W UV tubes (F8T5-BLB, 365 nm, 1.7 mW/cm²) and a Peltier device substrate cooling platform.

2.2. Preparation of microfluidic channels

Microfluidic channels were produced in cycloolefin copolymer (COC) wafers by hot embossing with micro-lithographic patterns of SU-8 photoresist on silicon wafers. Electrical conductors were produced on mating COC wafers by drawing lines with conductive carbon ink (Conductive Compounds Inc., type C-100 or in-house made mixture of 0.45 g glassy carbon powder and 0.05 g COC polymer in 0.7 mL methyl cyclohexane and 0.3 mL cyclohexane that was sonicated for 30 min until homoge-

nous) and then hot embossing the dried conductive lines into the surface with a hot and pressurized glass plate at 112.5 °C and 120 psi. Those carbon ink conductors are 1 mm wide and the actual electric resistance ranges from 5 to 6 Ω and 2.0 to 2.5 kΩ/mm for epoxy-based carbon ink and COC matrix carbon ink, respectively. The resulting COC wafer with conductors on a planar surface was bonded to the wafer with the embossed channels (which was exposed to saturated methyl cyclohexane vapor at room temperature for 1 min) to form a closed channel system having outlets at the edge of the device (40 °C, 200 psi, 10 min for bonding). The channels are 50 μm wide and 50 μm high for a 3 mm long emitter exit and 100 μm wide and 100 μm high for a 55 mm long monolithic column. Fused silica capillaries were sealed into the chips to make the connection between the columns and the HPLC mobile phase pumping system.

2.3. Preparation of polymeric monolithic columns

The details of the preparation of the monolithic columns are described by Ro et al. [31] elsewhere. The microfluidic channel walls were functionalized by photoinitiated graft polymerization to promote the bonding of the monolithic column to the channel [32,33]. In this work, the graft polymerization solution was made by mixing 30 μL of trimethylolpropane triacrylate, 70 μL of acetone, and 5 mg of benzophenone. The channels of the COC microchip were filled with the polymerization mixture and exposed to 365 nm UV light for 20 min at 25 °C. The functionalized channels were rinsed with acetone and dried with nitrogen. The channels were then filled with the monomer mixture to form a polymeric monolithic column in the channel. Poly-(ethylhexyl methacrylate-co-ethylene glycol dimethacrylate) (EHMA/EDMA) columns were prepared by polymerization of a monomer mixture consisting of 270 mg EHMA and 180 mg EDMA, porogenic solvent of 550 mg 1-decanol, and 3 mg of DPA as an initiator. The polymerization mixture was mixed ultrasonically into a homogenous solution and purged with nitrogen for 3 min. The two channels in the COC microchip were connected to the syringe using a MicroTee (Upchurch Scientific, Oak Harbor, WA) and filled with the mixture. Polymerization was initiated by UV irradiation for 20 min at 25 °C. There is a 1 mm gap between carbon electrode and monolith phase. After the polymerization was done, the monolithic column was rinsed with methanol for 12 h using a HPLC pump to remove unreacted monomers and porogenic solvents.

2.4. Surface modification

The exit edge of the chip was trimmed with a razor blade and placed in the vacuum chamber of an RF plasma cleaner (PDC-32G, Harrick Plasma, Ithaca, NY). The surface was cleaned in argon plasma for 1 min, and then treated with octafluorocyclobutane plasma for 3 min. Perfluoroalkyl ether (Krytox[®] 1625, Dupont, Wilmington, DE, USA) was applied to the fluorocarbon-coated edge to further enhance the hydrophobicity and durability around the edge openings. No effort was made to protect the channels from hydrophobic coating.

2.5. Instrument set-up

The carbon conductors are 1 mm wide and the front edge located 1.0 mm away from the exit. Electrospray potential (2.5 kV) was applied to the eluent in the emitter channel via the conductors in order to form ESI from the edge openings. The microfluidic device was mounted on a custom *X, Y, Z* adjustable source platform to optimize the emitter position for ESI. The spectra and chromatograms were acquired on a Finnigan LCQ Classic ion trap mass spectrometer. The integrated microchip for HPLC–ESI–MS was connected to the pumping system (Hewlett Packard 1100) to perform peptide separation and followed by ESI–MS detection. A PEEK tee (Upchurch Scientific) was connected after the HPLC pump and before an injection valve with a 1.0 μL sample loop, which typically achieved a 1 to 100 split of the flow to the column. The mobile-phase flow rate of the HP 1100 system was set at 30 $\mu\text{L}/\text{min}$ to keep the input flow rate for monolithic column at 300 nL/min. Mobile phase A was 5% acetonitrile in 0.1% aqueous TFA and mobile phase B was 70% acetonitrile in 0.1% aqueous TFA. The gradient was started at 0% B for 5 min, and ramped to 70% B in 60 min. One microliter of tryptic digested BSA (5 pmol/ μL) was injected from the injection valve onto monolithic columns. The data of chromatogram of BSA digest, full scan MS and data dependent MS/MS were processed with the Finnigan Xcalibur Qual Browser software package and exported to Microsoft Excel for evaluation.

To monitor the ESI processes and record Taylor cone images, the stainless steel sampling capillary was placed into a cylindrical black chamber. A Panasonic CCD camera (WV-BP332) attached via a 9.5 mm extension tube to a 4 \times microscope objective was mounted to capture the images through a hole on the chamber wall. A halogen fiber optic illuminator (MI-150, Dolan-Jenner, Lawrence, MA) was used to illuminate the spray. The microchip channel was coaxial with the MS entrance capillary with the fiber optic light beam and the optical axis of video camera perpendicular to this axis and to each other.

2.6. Protein digestion

BSA (1.0 mg) was dissolved into 1.0 mL NH_4HCO_3 solution (50 mmol). The BSA was reduced at 56 $^\circ\text{C}$ for 1 h by the addition of 460 mg of dithiothreitol (in 0.5 mL NH_4HCO_3 solution). The reduced protein was alkylated with 3.1 mg iodoacetamide in dark conditions at ambient temperature for 45 min. The alkylated BSA protein was precipitated in 10% trichloroacetic acid (TCA) water solution at 0 $^\circ\text{C}$ for 30 min. The precipitant was centrifuged and the supernatant was removed. The pellet was washed twice with double distilled water. The washed pellet was dissolved in 1.0 mL NH_4HCO_3 solution (50 mmol). Trypsin (10 mg in 50 mmol NH_4HCO_3 solution) was added and the protein was digested at 37 $^\circ\text{C}$ overnight. The digestion was quenched by addition of 10 μL TFA. The digest was diluted to 5 pmol/ μL using double distilled water to examine the overall analytical performances of the integrated chip by ESI–MS detection.

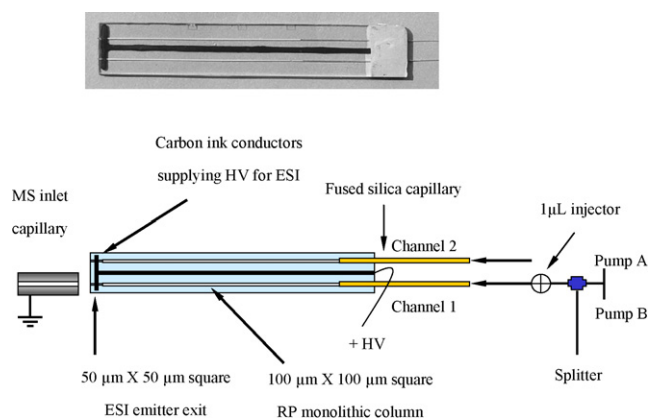


Fig. 1. Schematic diagram of the COC microfluidic device.

3. Results and discussion

3.1. Electrospray emitter array

The SU-8 photoresist master for hot embossing was produced on silicon wafers by micro-lithography [34]. To enhance the durability of SU-8 photoresist master, the microstructure was fabricated on a 30- μm thick planar photoresist film that was polymerized and covered the entire silicon wafer. The master was annealed at 180 $^\circ\text{C}$ for 30 min and allowed to cool to room temperature in the oven to relieve stress and increase the hardness of SU-8 epoxy. During heat treatment, the sharp edges of the microstructures were smoothed and rounded. However, the SU-8 mold can be used for only five to seven hot embossing processes due to gradual deformation. The ESI emitter array (shown in Fig. 1) was fabricated in COC wafers by hot embossing and solvent bonding. The sealed channel was able to resist more than 1000-psi pressure without leakage. The high voltage for electrospray ionization was applied through the carbon ink line. The carbon ink electrode (front edge located 1.0 mm away from the channel exits) is more stable than metals to electrochemical reactions, and significantly reduces resolution deterioration arising from electrochemical gas generation.

The hydrophobicity of the native COC surface is not high enough to maintain a stable electrospray ionization from the channel opening on the edge of the chip. RF plasma assisted chemical vapor deposition (RFCVD) with octafluorocyclobutane (C_4F_8) was tried first to modify the surface around the channel exit. A visible fluorocarbon polymer layer homogeneously coated the exit edge of emitter chip. During electrospray ionization, the hydrophobic surface surrounding the openings of the emitter chip restricts the Taylor cone bottom to the dimensions of the channel exit without accumulation of a resolution degrading droplet. This small Taylor cone improves the electrospray performance, thereby enhancing the detectability of ESI/MS. However, this thin fluorocarbon layer was damaged by occasional corona discharge leaving a visible ring of damage around the exit. As a result, the shape of the Taylor cone changed and the ESI performance (stability and efficiency) deteriorated. This problem was solved by adding a thin layer of perfluoroalkyl ether over the RFCVD coated

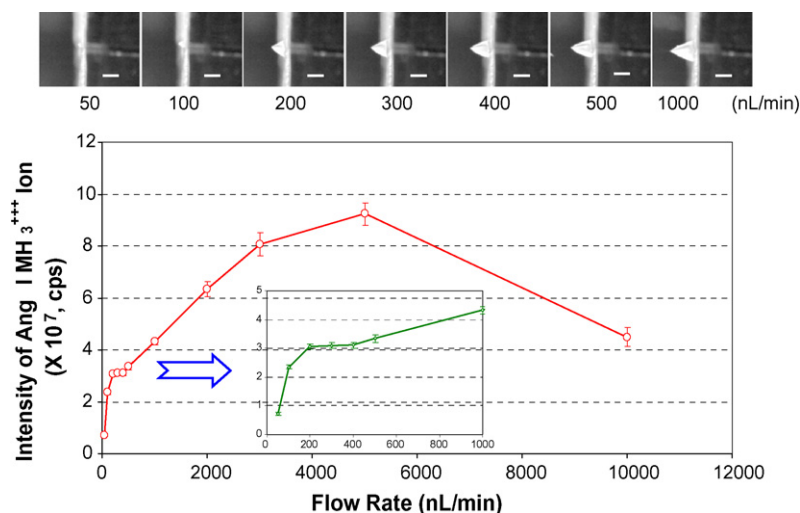


Fig. 2. Flow rate effects on the ESI ion intensity. The electrospray was generated at the voltage of 2.5 kV. Angiotensin I standard solution 100 fmol/ μ L in MeOH/H₂O/HAc (48:48:4, v/v/v) was infused by syringe pump. The distance from the emitter edge to the MS inlet capillary was 1.5 mm. The average signal intensities and the standard deviations were from 120 scans at m/z 433. The ESI images correspond to the different flow rates. The scale bar in the images equals 50 μ m.

fluorocarbon surfaces. The fluorocarbon covalently bonded to the COC surface serves as an anchor for the perfluoroalkyl ether, and the perfluoroalkyl ether becomes the sacrificial hydrophobic layer. This flexible layer has the ability to repair arcing damage and keep a complete hydrophobic surface around the edge exit. Lifetime of the resulting microfluidic emitter was over 20 h.

3.2. Flow rate effects on Taylor cone geometry and signal intensity

The design of the microfluidic ESI emitter array was aimed at integrating with multiple monolithic liquid chromatography columns on a single COC plastic chip for mass spectrometry analysis. The key factors in integrating the LC columns and ESI emitters are eluent flow rate and its influence on the Taylor cone geometry, that is critical to generating a stable and efficient electrospray. The eluent flow rate influence on ESI MS signal intensity was examined by infusing 100 fmol/ μ L Angiotensin I standard solution to the emitter array using a syringe pump. The emitter (without monolith phase) was able to generate stable electrospray in a wide range of flow rate (Fig. 2). At a low flow rate of 50–100 nL/min, the low signal intensity was apparently due to insufficient fluid supply. The Taylor cone base at this flow rate was narrower than the width of emitter exit. As the flow rate increased from 200 to 500 nL/min, the signal intensity of Angiotensin I significantly increased. However, there were no remarkable differences among those signal intensities. Comparing the ESI images, it can be seen that the Taylor cones were confined to the exit and the widths of Taylor cone bottom were equal to the width of emitter exit. The Taylor cone length increased with the flow rate. Further increases in the flow rate beyond 500 nL/min led to the Taylor cone expansion. When flow rate changed from 0.5 to 3.0 μ L/min, the signal intensity increased linearly. The ESI signal intensity reached a maximum at 5 μ L/min and decreased at 10 μ L/min. The ESI signal intensity was proportional to the width of Taylor cone

base when the flow rate was lower than 5 μ L/min. This ESI emitter array can be operated over the range of 50 nL/min to 10 μ L/min. The most stable electrospray was achieved with the flow rate from 200 to 500 nL/min, which is suitable for monolithic or packed capillary column LC–MS analysis. It should be noted that the triply charged Angiotensin ions were the dominant ion species in the spectrum. This pattern did not change with the flow rate increasing from 0.050 to 10 μ L/min.

3.3. ESI voltage influences on signal intensity

The ESI voltage applied to the emitter array ranged from 2.0 to 2.9 kV, which is lower than commonly used ESI potentials. In this range, the distribution of three charged species and the signal-to-noise ratio were rather stable, and the voltage has little influence on the mass spectrometric signal intensity (see Fig. 3). If the voltage between the emitter conductor and MS sampling capillary is lower than 2.0 kV, the emitter cannot sustain stable ESI. When the ESI voltage is higher than 2.9 kV,

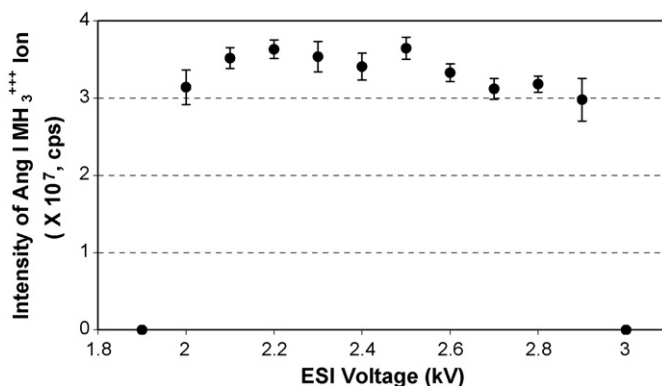


Fig. 3. Voltage effects on the ESI ion intensity. The electrospray was operated at the flow rate of 300 nL/min. The distance from the emitter tip to the capillary was 1.5 mm. The average signal intensities and the standard deviations were from 120 scans at m/z 433.

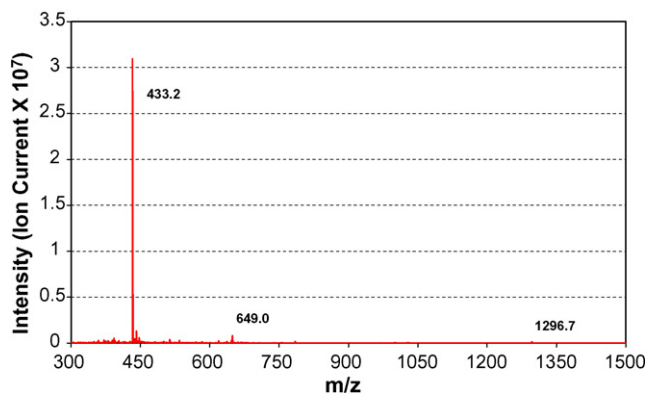


Fig. 4. The mass spectrum obtained with carbon ink conductor emitter. Angiotensin I standard solution 100 fmol/ μ L in MeOH/H₂O/HAc (48:48:4, v/v/v) was infused through the emitters at the flow rate of 300 nL/min. The ESI voltage was 2.5 kV. Two hundred scans were accumulated for this spectrum.

discharge occurs between MS sampling capillary and carbon ink conductor. This arcing quickly damages the carbon ink conductor and the hydrophobic fluorocarbon layer around the emitter exit resulting in degradation of the ESI performance of the emitter. Low electrical resistance of the epoxy-based carbon ink conductor appeared to facilitate the direct discharge between MS sampling capillary and emitter conductor. This suggested that increasing the electrical resistance of carbon ink conductor could reduce this discharge. The average electrical resistance of the in-house made carbon ink was 400 times higher than the commercial carbon ink. Use of this ink for the carbon electrode allowed stable operation in the potential range between 1.8 and 4.0 kV without significant corona or arcing. Bubble generation around the conductor was also effectively inhibited. Therefore, doping glassy carbon spherical powder into COC wafer is a favorable method to produce the electric conductor. It not only has the same COC surface as chip substrate, but also provides

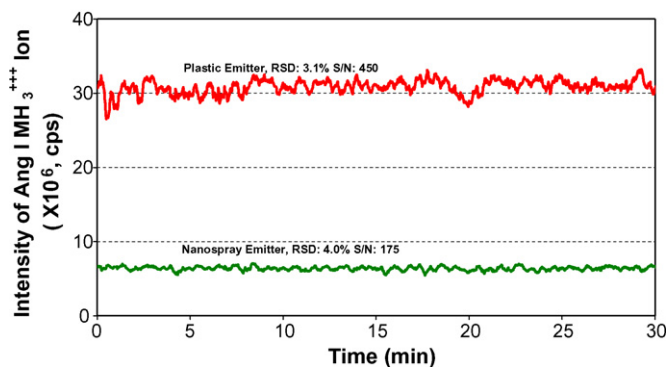


Fig. 5. Comparison of the signal sensitivity and stability of the electro-spray ionization between plastic emitter (upper trace) and the commercial nanospray emitter (lower trace). Angiotensin I standard solution 100 fmol/ μ L in MeOH/H₂O/HAc (48:48:4, v/v/v) was infused through the emitters at the flow rate of 300 nL/min. The ESI voltage was 2.5 kV (plastic emitter) and 1.9 kV (New Objective nanospray emitter).

stable electrospray ionization. In the experiments described below, the ESI voltage was set at 2.5 kV.

3.4. Performance of the microfluidic emitter array

Spectrum background, detectability, and signal stability are the most important factors to evaluate the performances of the ESI microfluidic emitter device. The carbon ink conductor did not appear to introduce any impurity into the mass spectrum. The distribution of three charged species were rather stable. In comparing the plastic emitter and the conventional nano-emitter, both gave a very clean background (see Fig. 4).

The detectability and stability of the emitter array have been compared to a commercial New Objective nano-emitter (FS360-50-8-CE) at a flow rate of 300 nL/min. The electrospray ionization was carried out under the optimized conditions for each emitter. The long-term stability of two kinds of emitters is com-

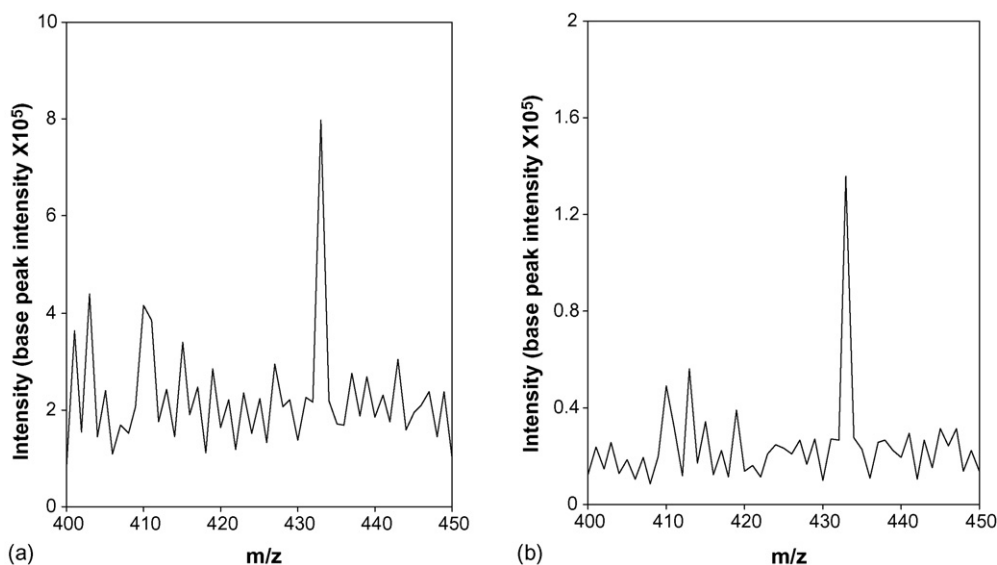


Fig. 6. Comparison of the detection sensitivity of the plastic emitter and a conventional nano-emitter at low peptide concentration. Angiotensin I concentration was 10 fmol/ μ L and infused with syringe pump at the flow rate of 300 nL/min. The ESI voltage applied to (a) plastic emitter (2.5 kV) and (b) New Objective nanospray emitter (1.4 kV) was optimized for each emitter. Two hundred scans were averaged to collect these spectra.

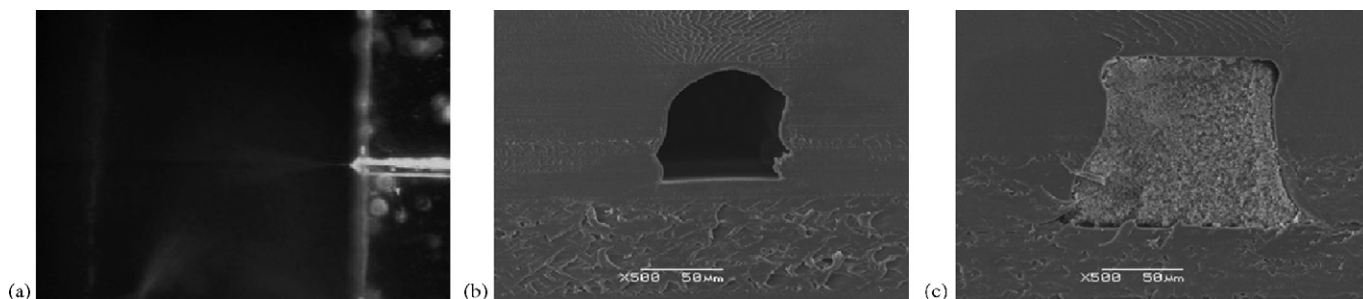


Fig. 7. (a) Image of a stable ESI process, (b) SEM micrograph showing the cross section of emitter exit, and (c) SEM micrograph showing the excellent covalent bonding between monolith stationary phase and the microchannel.

parable. However, the plastic emitter gave nearly 5 times more signal and 2.5 times higher signal to background ratio than the conventional nano-emitter in this comparison (see Fig. 5). After the concentration of Angiotensin I was gradually diluted down to 10 fmol/ μ L, the signal intensity achieved using plastic emitter was still five times higher than nano-emitter with the similar signal to background ratio (see Fig. 6).

The glassy carbon/COC carbon ink conductor is durable. If operated properly, each emitter of this array can be used for more than 20 h. Arcing between carbon ink conductor and the sampling capillary of MS is the main reason for degradation. The long lifetime makes this emitter design amenable to interfacing LC and MS for collecting reliable MS and MS/MS data. In our experiments, one microfluidic chip run 4 days and 7 h per day were normal.

3.5. Monolithic column LC–MS performance

In polymerizing the monolithic columns in this microfluidic device, commercial epoxy-based carbon ink cannot be used as the electrical conductor because it is soluble in acetone, one of the solvents used for the monolithic column preparation. The in-house made COC-based carbon ink is resistant to polar solvents such as acetone, methanol, and isopropyl alcohol. Another advantage is that the chemical properties of the COC plate and the surface of COC-based carbon ink are very similar. When solvent enhanced thermal pressure bonding took place between bottom plate and cover plate, the carbon ink conductors were completely sealed, which avoided any gaps or leakages that can occur between COC wafers and epoxy-based carbon ink conductors.

In this microfluidic device, the reverse phase liquid chromatography is directly followed by ESI generation reducing post-column diffusion which could degrade resolution. The UV transparency of COC enables UV-initiated photopolymerization of the monolithic columns. In this work, the end of the monolithic stationary phase was 1 mm from the carbon ink conductor line. The ($50\ \mu\text{m} \times 50\ \mu\text{m}$) channel length from the end of the monolith to the exit was 3 mm long giving a post-column volume (dead volume) of about 7.5 nL. With a mobile phase flow rate of 300 nL/min, the eluent will be electrosprayed 1.5 s after the LC separation. This short time, plus the laminar flow conditions in the $50\ \mu\text{m} \times 50\ \mu\text{m}$ channel minimizes post-column resolution degradation of the monolithic column LC separation.

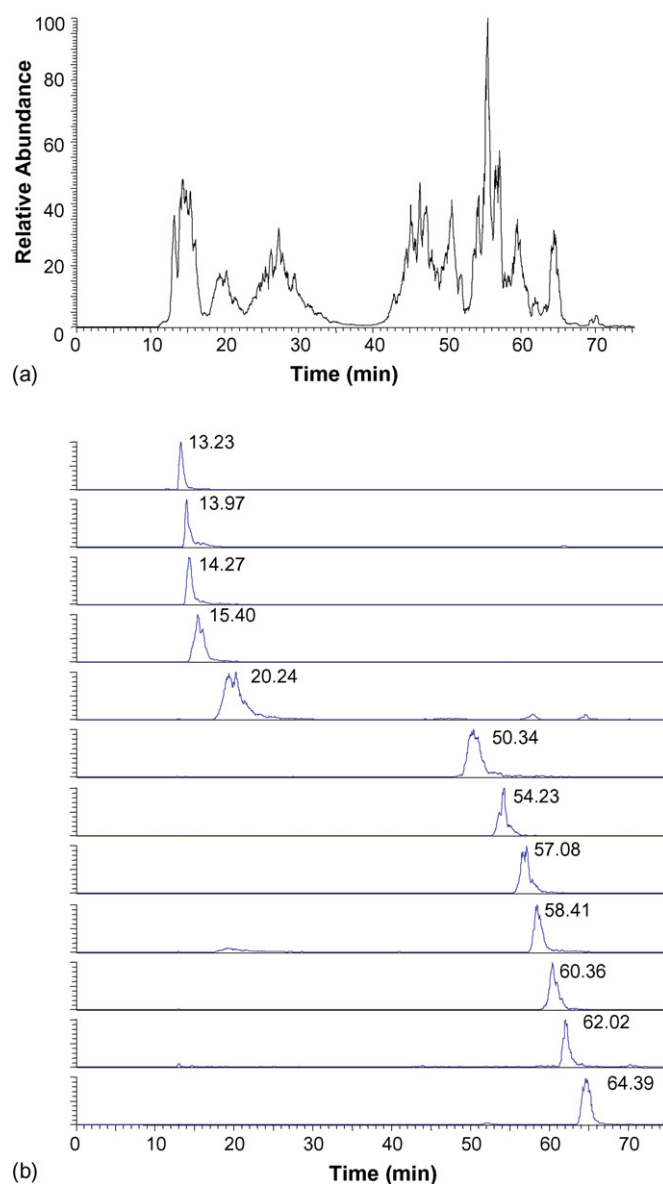


Fig. 8. Chromatogram (a) and extracted peptide ion chromatograms (b) from the monolithic column microchip LCQ–ESI–MS analysis of tryptic digested BSA (5 pmol). SEQUEST database searching shows the amino acid sequence coverage was 70%.

The COC microfluidic device was sealed by a solvent-enhanced thermal pressure bonding method yielding a device that can withstand over 1000 psi pressure without leaking. After functionalization of the channel walls by graft polymerization, the porous polymer monolithic columns were polymerized in situ using UV irradiation with a photomask to confine the porous polymer monolith to the desired regions of the channels. The monolithic stationary phase was homogenous and well bonded to the COC channel surfaces. An image of the stable ESI process and SEM micrographs of emitter exit cross section and the covalent bonding between monolith stationary phase and the microchannel wall are shown in Fig. 7.

After the preparation of monolithic column, the exit edge of the chip was trimmed with a razor blade. The fresh COC surface was treated in octafluorocyclobutane plasma for 3 min. Then, the fluorocarbon-coated edge was painted with perfluoroalkyl ether to enhance the hydrophobicity around the edge openings. The performance of the device was demonstrated by analysis of a tryptic digest of bovine serum albumin on a Finnigan LCQ ion trap MS instrument using a gradient mobile phase for the peptide separation. Extremely stable electrospray ionization was achieved throughout the chromatographic separation. The separation efficiency of the monolithic column is shown in the chromatogram and in the extracted peptide ion chromatograms in Fig. 8. The Half peak width ranged from 0.44 to 2.25 min.

4. Conclusion

This work demonstrates that stable and sensitive ESI can be achieved with an emitter consisting of a simple channel opening at the edge of a plastic microfluidic device. Treatment of the surface surrounding the channel opening with a fluorocarbon film confines the Taylor cone to the channel opening, which restricts the liquid effluent from spreading out over the device edge. The use of high resistance carbon ink, which can be easily printed and hot embossed, as an electric conductor gave superior performance compared to conventional carbon ink or noble metal electrodes in terms of resistance to electrical discharge. No detectable impurities were observed in the spectrum background from the electrodes. This plastic emitter offers a sensitive, stable, and long lasting ESI-MS enabling practical coupling to a monolithic column as an integrated microfluidic device for reversed phase LC separation directly followed by ESI-MS analysis. The flow rate operating range of the emitter fully met the requirement of the chromatography. The dead volume of the emitter exit was negligible, minimizing post-column resolution degradation. The performance of this microfluidic device in analysis of a tryptic digest mixture indicated the design was adequate for further work in which the column/ESI emitter array will be expanded to larger numbers and integrated with a first dimension ion exchange separation column to produce a 2D LC-ESI-MS device.

Acknowledgments

This work was supported in part by NIH grant CA86285 and the NHLBI Proteomics Initiative via contract N01-HV-28181.

References

- [1] M.S. Wilm, M. Mann, *Int. J. Mass Spectrom. Ion Process.* 136 (1994) 167–180.
- [2] M.R. Emmett, R.M. Caprioli, *J. Am. Soc. Mass Spectrom.* 5 (1994) 605–613.
- [3] D.C. Gale, R.D. Smith, *Rapid Commun. Mass Spectrom.* 7 (1993) 1017–1021.
- [4] S. Nilsson, M. Svedberg, J. Pettersson, F. Björefors, K. Markides, L. Nyholm, *Anal. Chem.* 73 (2001) 4607–4616.
- [5] K.B. Mogensen, H. Klank, J.P. Kutter, *Electrophoresis* 25 (2004) 3498–3512.
- [6] W. Sung, H. Makamba, S. Chen, *Electrophoresis* 26 (2005) 1783–1791.
- [7] T.T. Razunguzwa, J. Lenke, A.T. Timperman, *Lab on a Chip* 5 (2005) 851–855.
- [8] J. Xie, Q. He, Y. Tai, J. Liu, T. Lee, *Proceedings of the 16th IEEE Annual International Conference on Micro-Electro Mechanical Systems, Kyoto, Japan January 19–23, 2003*, pp. 443–446.
- [9] J. Xie, Y. Miao, J. Shih, Q. He, J. Liu, Y. Tai, T.D. Lee, *Anal. Chem.* 76 (2004) 3756–3763.
- [10] L. Licklider, X. Wang, A. Desai, Y. Tai, T.D. Lee, *Anal. Chem.* 72 (2000) 367–375.
- [11] S. Le Gac, S. Arscott, C. Cren-Olivé, C. Rolando, *J. Mass Spectrom.* 38 (2003) 1259–1264.
- [12] S. Arscott, S. Le Gac, C. Druon, P. Tabourier, C. Rolando, *J. Micromech. Microeng.* 14 (2) (2004) 310–316.
- [13] J. Kameoka, R. Orth, B. Ilic, D. Czaplewski, T. Wachs, H.G. Craighead, *Anal. Chem.* 74 (2002) 5897–5901.
- [14] Y. Yang, J. Kameoka, T. Wachs, J.D. Henion, H.G. Craighead, *Anal. Chem.* 76 (2004) 2568–2574.
- [15] C.H. Yuan, J. Shiea, *Anal. Chem.* 73 (2001) 1080–1083.
- [16] T.C. Rohner, J.S. Rossier, H.H. Girault, *Anal. Chem.* 73 (2001) 5353–5357.
- [17] P. Lozano, M. Martínez-Sánchez, J.M. Lopez-Urdiales, *J. Colloid Interface Sci.* 276 (2004) 392–399.
- [18] T. Koerner, K. Turck, L. Brown, R.D. Oleschuk, *Anal. Chem.* 76 (2004) 6456–6460.
- [19] Q. Xue, F. Foret, Y.M. Dunayevskiy, P.M. Zavracky, N.E. McGruer, B.L. Karger, *Anal. Chem.* 69 (1997) 426–430.
- [20] Y. Wang, J.W. Cooper, C.S. Lee, D.L. DeVoe, *Lab on a Chip* 4 (4) (2004) 363–367.
- [21] K. Tang, Y. Lin, D.W. Matson, T. Kim, R.D. Smith, *Anal. Chem.* 73 (2001) 1658–1663.
- [22] M. Schilling, W. Nigge, A. Rudzinski, A. Neyer, R. Hergenroeder, *Lab on a Chip* 4 (3) (2004) 220–224.
- [23] S.S.J. Jeyaprasath, D. Steger, R. Birkle, G. Zengerle, R. Koltay, P. Rühel, *J. Anal. Chem.* 77 (2005) 6469–6474.
- [24] M. Wetterhall, O. Klett, K.E. Markides, L. Nyholm, J. Bergquist, *Analyst* 128 (2003) 728–733.
- [25] A.P. Dahlin, M. Wetterhall, G. Liljegren, S.K. Bergström, P. Andrén, L. Nyholm, K.E. Markides, J. Bergquist, *Analyst* 130 (2005) 193–199.
- [26] A.J. Link, J. Eng, D.M. Schieltz, E. Carmack, G.J. Mize, D.R. Morris, B.M. Garvik, J.R. Yates III, *Nat. Biotechnol.* 17 (1999) 676–682.
- [27] D.A. Wolters, M.P. Washburn, J.R. Yates III, *Anal. Chem.* 73 (2001) 5683–5690.
- [28] Y. Yang, C. Li, J. Kameoka, K.H. Lee, H.G. Craighead, *Lab on a Chip* 5 (2005) 869–876.
- [29] J. Carlier, S. Arscott, V. Thomy, J.C. Camart, C. Cren-Olivé, S. Le Gac, *J. Chromatogr. A* 1071 (2005) 213–222.
- [30] H. Yin, K. Killeen, R. Brennen, D. Sobek, M. Werlich, T. van de Goor, *Anal. Chem.* 77 (2) (2005) 527–533.
- [31] K.W. Ro, J. Liu, D.R. Knapp, *J. Chromatogr. A* 1111 (2006) 40–47.
- [32] B. Rånby, *Mater. Res. Innovat.* 2 (1998) 64–71.
- [33] T. Rohr, D.F. Ogletree, F. Svec, J.M. Fréchet, *J. Adv. Funct. Mater.* 13 (2003) 264–270.
- [34] J. Zhang, K.L. Tan, H.Q. Gong, *Polym. Test.* 20 (2001) 693–701.